Recent increase in a recurrent Pan-Atlantic wave-pattern driving concurrent wintertime extremes

Kai Kornhuber[1], Gabriele Messori[2,3]

[1]Earth Institute, Columbia University, New York, NY, USA
[2] Dept. of Earth Sciences and Centre of Natural Hazards and Disaster Science (CNDS), Uppsala University, Uppsala, Sweden
[3]Dept. of Meteorology and Bolin Centre for Climate Research, Stockholm University, Stockholm, Sweden

This is a non-peer reviewed version of a manuscript accepted at BAMS

Abstract

Wintertime extremes such as cold spells and heavy precipitation events can have severe societal impacts, disrupting critical infrastructures, traffic and affecting human well-being. Here, we relate the occurrence of local and concurrent cold or wet wintertime extremes in North America and Western Europe to a recurrent, quasi-hemispheric wave-4 Rossby wave jet-pattern. We identify this pattern as a fundamental mode of Northern Hemisphere (NH) winter circulation, and one which exhibits phase-locking behavior. Thus, the associated atmospheric circulation and surface anomalies re-occur over the same locations when the pattern's wave amplitude is high. The wave pattern is strongest over the pan-Atlantic region, and is associated with an increased probability of extreme cold or wet events by up to 300 % in certain areas of North America and Western Europe. The pattern has increased significantly in frequency over the past four decades (1979-2021), which we hypothesise may derive from increased convective activity in the tropical Pacific, from where the pattern originates. The identified pattern and its remote forcing might provide pathways for early prediction of local and concurrent cold or wet wintertime extremes in North America and Western Europe.

1 Introduction

Climate extreme events can have major socioeconomic impacts causing substantial damage to infrastructure and property and negatively affect human well-being (e.g. Hales et al., 2003; Forzieri et al., 2018; Smith & Sheridan, 2019; MunichRe, 2020; **?**). Cold-season high-impact events include cold spells and rain-driven floods, which may disrupt traffic and supply chains (e.g. Vajda et al., 2014), the energy sector (e.g. Doss-Gollin et al., 2021; Busby et al., 2021) and pose a high risk for lower income communities and the homeless (e.g. López-Bueno et al., 2020). Recent examples include the 2021 Texas cold spell or the 2019 North American (NA) east coast cold spell. Although the severity of cold spells is projected to decrease under continued global warming Screen (2014), cold extremes will continue to be a major climate hazard for the coming years (Gao et al., 2015). Next to cold spells, wintertime heavy rainfall and the associated flooding has caused widespread damage. Examples include the severe 2019–20 U.K. floods and the 2020 floods in Spain and France associated with the winter storm Gloria (Sefton et al., 2021; Amores et al., 2020). Although recent trends in flood hazards display considerable regional variability Blöschl et al. (2017), climate projections suggest widespread increases in heavy winter rainfall over large parts of Europe Scoccimarro et al. (2013); Rajczak & Schär (2017), coupled with an increase in complex compound hazards such as rain-on-snow flooding events Musselman et al. (2018).

Recurrent, persistent patterns that favour the occurrence of wintertime extremes in specific regions are of particular interest in the context of timely prediction and for understanding associated physical mechanisms. Large meridional meanders of the tropospheric jet stream, diagnosed as blocking patterns Woollings et al. (2018) or as amplified Rossby waves (in case of more zonally elongated ridge-trough patterns **??**Screen & Simmonds (2014); Grotjahn et al. (2016)) are key atmospheric dynamical drivers of weather extremes in the mid-latitudes. Some wave-patterns exhibit preferred phases and are thus recurrent with respect to the locations of ridges and troughs and associated surface anomalies **?**Kornhuber et al. (2019, 2020). Such recurrent patterns are supposedly enforced by zonal asymmetries of the earth's surface (cite) imposed by mountain ridges, land-ocean boundaries and sea-surface temperature anomalies (cite). These stationary forcing patterns promote preferred phases for certain waves which can provide opportunities for predicting associated extreme weather events Teng et al. (2013); Harnik et al. (2016).

Due to their zonal extent, amplified Rossby waves are often associated with concurrent weather extremes at geographically remote locations (e.g. Teng et al., 2013; Harnik et al., 2016; Kornhuber et al., 2019, 2020). Such spatially compounding extremes are of particular interest due to their potentially enhanced impacts compared to extremes occurring in isolation Zscheischler et al. (2020); Raymond et al. (2020); Kornhuber et al. (2020). Here, we investigate recurrent Rossby waves in the extended northern hemisphere (NH) winter season (November-March) following the approach outlined in Kornhuber et al. (2020) for the summer season. We investigate the large-scale circulation during the recent 2019 cold spell (Sect. 3.1) and identify wave-4 as a recurrent wave pattern which was linked to several cold extremes in North America and cold or wet extremes in Europe in recent years (Sect. 3.2). We quantify its role in driving local cold or wet extremes and their concurrence in North America and Europe (Sect. **??**) and conclude with a discussion of recent trends and its association with dominant modes of climate variability (Sect. **??**).

2 Data and Methods

2.1 Data

The analysis is based on ERA5 reanalysis (1979-2020) (Hersbach et al., 2020), with a horizontal spatial resolution of 0.5° (for temperature and precipitation) and 1° for meridional winds. The analysis focuses on the extended NH cold season (November to March, NDJFM). The data is aggregated from hourly (6-hourly) surface (pressure-level) values to daily values prior to analysis. Temperature and precipitation anomalies are defined relative to a daily climatology, computed using a time-series smoothed with a 15-day running mean. Precipitation anomalies are further averaged over a 9-day window. Extreme temperature and precipitation events are defined as values in the top or bottom 5 percentiles of the respective anomaly distributions. In all figures, statistical significance is computed using a random sampling procedure with 1000 iterations, at the 5% one or two-sided significance level.

Timeseries of monthly values of dominant modes of variability such as the Atlantic Arctic Oscillation index (AAO), the North-Atlantic Oscillation (NAO), the Arctic Oscillation (AO), the El Nino Southern Oscillation 3.4 (ENSO), the Pacific North American pattern (PNA) and the Pacific Decadal Oscillation (PDO) were retrieved from NOAA.

2.2 Methods

2.2.1 Definition of Wave amplitude and wave phase Events

Wave amplitudes and phases are based on a fast Fourier decomposition, by applying the function 'fft' from the R-package 'stats' (cite) on weekly means of the 250 hPa mean meridional wind, averaged at each longitude over [37.5° N-57.5° N], following the approach of in Kornhuber 2020 Kornhuber et al. (2020).

To highlight its robustness, we follow two complementary wave event definitions for the wave-4 pattern: A *wave amplitude event* is identified as a week when the amplitude of wave-4 is at least 1.5 standard deviations above the mean monthly climatological value within NDJFM. This definition yields 82 events. Note that a high wave-amplitude does not necessarily refer to an extraordinarily large North–South extension of a jet meander, but rather means that the meridional (North–South) wind velocity is high. While wave amplitude events make no a priori assumption about the waves longitudinal location (i.e. the location of ridges and troughs), *wave phase event* are more directly linked to the wave-4 pattern's preferred phase. We first compute the spatial correlation of 7-day running mean meridional wind fields over the NA – European sector [160° W – 40° E, 30 – 72.5° N]. We then identify days on which the correlation exceeds the 90th percentile of the full distribution, select local maxima in the case of exceedance on several consecutive days and finally impose a minimum 10-day separation between successive local maxima. This minimises event aliasing and confounding influences from auto-correlation, and yields a total of 103 *wave phase events*.

2.2.2 Analysis of Extreme Weather and its Concurrence

To quantify whether wave-4 events favour extreme events, we compute an extreme event ratio which is the extreme event frequency at each grid-point normalised by the climatological frequency of extreme events at a particular location (5% according to the definition we use here). Thus, a value of one at a given location indicates no effect of the wave-4 events on extreme event frequency, while a lower value indicates fewer extremes and a value above one indicates a favourable effect for extremes to occur. To quantify the co-occurrence of extreme events in NA and Europe we introduce the extremes concurrence index (ECI). For every gridpoint and wave event (Sect. 2.2.1) in NA [160 – 40° W, 30 – 72.5° N] we count how many gridpoints in Europe [40° W – 40° E, 30 – 72.5° N] display a concurrent extreme event during each of the 5 days centred on the peak of the wave event. We then weigh by gridpoint area and normalise over [0 1] to obtain a spatial compounding index. The same process is repeated for every gridpoint in Europe, while considering extreme events in NA. The value assigned to each gridpoint is the ECI value composited across all wave events. Thus, high values of ECI at a given gridpoint in Europe (NA) indicate co-occurrence of extreme events between that location and gridpoints in NA (Europe). We exclude Greenland and Iceland are not included in the calculation. ECI values are computed for locations that exhibit where identified to experience an increased frequency of extremes during wave events following the location based extreme event ratio.

3 Results

3.1 The concurrent 2019 NA and Scandinavian cold-spells

A severe cold spell affected the mid-western United states and Canada at the end of January 2019, with record low temperatures approaching -40C degrees measured at a local station on Mount Carrol, Ilinois (cite NOAA). The record cold and heavy snowfall heavily affected supply chains and traffic by blocking roads and disrupting train lines and air traffic. A total of 21 fatalities were reported, several of which from hypothermia (cite). Within the same week, Sweden recorded a temperature of -39 C in Northern Lapland. Investigating the large-scale circulation we find that the cold waves in North America and Europe were connected by a wave pattern in the upper tropospheric mid.latitude circulation that arched over the Atlantic (Fig. 1a) and is diagnosed as an amplified (Fig.1b), phase-locked wave-4 pattern, remaining in place for well over a week (Fig.1c). We find that these connected extremes where yet another example of a specific wave-regime that was linked to other cold extremes in the past such as the 2013 and 2018 wintertime cold extremes (see SI Fig. 1, 2)

From the XX events we identify several are linked to record breaking cold events such as the recent cold-waves over NA and Europe in winters XX, XX, XX (ADD: Figure or table showing all detected events for SI). [Provide Dates / Add List to SI??]

3.2 A recurrent wavenumber 4 pattern in the northern hemisphere Winter circulation

Wave-4 constitutes a recurrent pattern in the Northern hemisphere winter circulation. The recurrence of the pattern is defined by a close relationship of the waves amplitude and its phase (Fig. 3.2), i.e. the phase position of the wave converges towards a preferred value with increasing amplitude. Such phase-locking behaviour was found for wave 5 and 7 in Summer (June–August; Teng et al. (2013); Kornhuber et al. (2020); **?**), but for winter (NDJFM) this behaviour is a unique feature of wave-4 for synoptic scale waves in the northern hemisphere mid-latitudes. While waves 5 and 6 exhibit a single peak in their probability density the range of the 25th - 75th percentile around the median is wider (grey hatched area in Fig. 2) during wave amplitude events and exceeds pi/2 (the threshold for phase locking defined in Kornhuber et al. (2020). In consequence, a well organised pan-Atlantic pattern emerges in the 250 hPa meridional wind and 500 hPa geopotential height fields (Fig. 3a, b) when sampling for wave amplitude events (Sect. 2.2.1) (see Fig. XX for wave phase events). Note that the meridional wind and geopotential height composites are conditioned on amplitude events alone and not filtered by a specific phase. The pattern exhibits strongest features over Northern America and Europe, and seemingly emanates from tropical Pacific. The geopotential height ridge over NA is co-located with the Rocky Mountains, forming a dipole of high and low pressures over the continent. This is followed further downstream by a ridge that spans across the North Atlantic. A weaker pattern of ridges and troughs is visible over central Asia a region where the Atlantic storm track often splits into polar and a subtropical jets.

Surface temperature and precipitation anomalies follow the position of ridges and troughs over NA and Europe (Fig. 3c, d). The strongest temperature anomalies occur over NA, where the presence of a southerly flow anomaly in the western part of the continent and a corresponding northerly flow further to the east lead to a zonal temperature anomaly dipole with a magnitude of roughly 6 K across the continent. This is akin to the intensified NA winter dipole reported by Singh et al. (2016). Western Europe displays weaker, yet regionally significant, cold anomalies associated with an anomalous northerly flow. Cold wintertime spells over Europe are primarily associated with easterly or northeasterly air flows (e.g. Sillmann et al., 2011), explaining the weaker surface temperature footprint of the wave pattern in particular for central Europe.

Cold anomalies over NA are predominantly dry, while in Europe there is a partial overlap between the region of significant cold anomalies and a region of positive precipitation anomalies (Fig. 3c,d). Indeed, the precipitation anomalies are roughly aligned with the near surface temperature anomalies over eastern NA, where the northerly flow advects cold, dry air masses. In Europe, respective anomalies exhibit a zonal dislocation which may be explained through the effect of topography and land-sea contrasts on precipitation. The stronger meridional wind component likely reduces zonal advection of moist oceanic air, leading to negative precipitation anomalies in western Iberia and the British Isles. Further east, in areas where the Mediterranean Sea provides an important moisture source for wintertime precipitation (Ciric et al., 2018), the wave pattern leads to positive precipitation anomalies.

3.3 Local and concurrent weather extremes in Europe and NA are amplified by a wave-4 pattern

The probability of local cold extremes is increased by a factor of up to three during the occurrence of a wave-4 phase event. Here we analysis wave-4 phase events defined by the v-wind pattern correlation over the NA and European sector (see black box in Fig. 3a) and Sect. 2.2.1. For an analysis based on wave amplitude events see Fig. SI which show qualitatively similar results). The NA east coast is particularly affected by extreme cold spells (Fig. 3.3a) where their occurrence is significantly increased along the entire coastline from 30° N to beyond the Arctic circle. The probability of cold spells in Europe is amplified strongest in South-Western Europe and Scandinavia, with increase of a factor 2 . Precipitation extremes are favoured as well, with strongest signals over central Europe and Eastern Europe Fig. 3.3b where the likelihood of wet extremes is amplified by a factor of beyond three in some regions.

We further analyse the wave effect on the co-occurrence of cold extremes (Fig. 3c) and cold and wet extremes (Fig. 3d). Using the ECI diagnostic (Sect. 2.2.2) we find that the co-occurrence of cold extremes experiences a significant increase across eastern NA and western and southern Europe (Fig. 3.3c). Similar results are found for extreme cold events in NA and wet events in Europe (Fig. 3.3c), however affected regions are shifted to the North and East mirroring the pattern identified for local precipitation extremes (Fig. 3.3b). The amplified concurrence identified on both continents provides further evidence that the wave-pattern identified in the upper level circulation (Fig. **??**a, b) is not a product of separate local ridges that occur independently owing their coherent pattern seen in composites **??** to the applied averaging, but is in fact a pan Atlantic regime-like feature favouring the co-occurrence of surface extremes on daily to weekly time-scales.

3.4 Recent trends and remote forcing

Analysing trends in mean wave-4 amplitude, wave-amplitude events and phase velocity we find a significant increase in amplitude and events and a decreasing, however non-significant trend in phase velocity over the observational period NDJFM 1979–2020 (Fig. 5a). The positive trends in amplitude and wave amplitude events is in agreement with Singh et al. (2016), who found an increase in the occurrence of a winter dipole over NA, which regionally matches patterns associated with a high amplitude wave-4. Wave phase events however do not exhibit an increasing trend (Fig. SI). This is explained by the fact, that the correlation based metric is less sensitive to the wave-amplitude (i.e. the strength of the ridge) but more sensitive to the waves phase, which shows no significant change over the past decade (not shown).

The presence of a large-scale, phase-locked and recurrent pattern driving regional extreme events may be exploited in the context of predictability, e.g. Harnik et al. (2016) showed that circumglobal wave-patterns can provide medium-range predictability for NA cold spells, and the broader role of wave patterns or packets as drivers of concurrent extreme events and predictability tools has been discussed in a number of studies (e.g. **?**Wirth et al., 2018; Kornhuber et al., 2020; Fragkoulidis & Wirth, 2020, and references therein). To identify potential drivers of the increasing trend we investigate the relationship of monthly wave amplitude and spatial correlation with dominant modes of climate variability monthly values of the Atlantic Arctic Oscillation index (AAO), the North-Atlantic Oscillation (NAO), the Arctic Oscilation (AO), the El Nino Southern Oscillation (ENSO), the Pacific North American pattern (PNA) and the Pacific Decadal Oscillation (PDO). Further we investigate the relationship of the pattern to the meridional temperature gradient as defined by the difference of temperatures averages of higher latitudes (70deg. N - 90deg. N) and lower latitudes (50deg N 30deg N) following the definition in **??**. For the indices that relate to pacific variability (ENSO, PNA, PDO) however we find strongest and partly significant relationships (ref FIG). For wave amplitudes we find significant relationships for ENSO and PDO in December, for ENSO in March and for PNA in November. Significant relationship for November to January are found for PNA and for November and December for PDO for spatial correlation across the North American - European sector and the mid.latitude belt. Patterns associated with the Atlantic circulation show mostly insignificant correlations, except for the NAO and the AO in January for the North American - European sector. The meridional temperature gradient, however exhibits no notable correlation. We thus conclude that is a potential remote forcing that acts on the occurrence of wave-4 events is located in the pacific and that positive trends in wave amplitude and events might be linked to increased convection in this area (cite).

4 Discussion and Conclusions

Although a decrease in the severity and frequency of cold-spells is expected in a warming world based on thermodynamical arguments, atmosphere dynamical changes, could potentially lead to an increase in northern hemisphere cold-extremes (cite). Irrespective of long term trends, cold extremes and their impacts will remain a significant hazard in the coming decades Gao et al. (2015) for instance through false spring events, that can have severe impacts on orchards and harvests. Recent studies have emphasised the stratospheric polar vortex as a driver of mid-latitude cold extremes (Matthias & Kretschmer, 2020; Cohen et al., 2021) e.g. a weakened polar vortex Kretschmer et al. (2018), Arctic Amplification Cohen et al. (2014), and changes in jet stream sinuosity or wave activity (e.g. Screen & Simmonds, 2014; Cattiaux et al., 2016; Martin, 2021) has sparked a lively discourse in the scientific community, which is still ongoing Barnes & Screen (2015); Cohen et al. (2020).

We identified a quasi-hemispheric wavenumber 4 pattern which modulates the occurrence of wintertime extreme events in NA and Europe. Due to its phase-locked behaviour and recurrence, the extremes associated with the pattern occur repeatedly in the same geographical regions. These include cold spells in eastern NA and cold or wet spells in Europe. Due to the wave pattern's large zonal extent, these extreme events on the two sides of the North Atlantic occur largely synchronised. We find an increase in wave 4 amplitude and wave- 4 events which does not seem to be linked to the meridional temperature gradient but seems to be linked to the pacific. The wave-4 pattern here has only a weak correlation to canonical climate modes of variability in the Atlantic, but significant correlations with those that relate to Pacific variability. Next steps will involve the systematically analysis of the origin of the wave pattern and atmosphere dynamical mechanisms that lead to its recurrence and persistence. This could then be used to build a statistical predictor for co-occurring regional wintertime extremes or to better understand the performance of numerical weather predictions for some extreme event case-studies. Future work will also investigate if identified trends in the wave-4 pattern are reproduced by historical climate model simulations and if they are projected to continue in simulations based on future emission scenarios to investigate its relation to anthropogenic climate change and future risks from extreme cold spells.

Further talking points:

1. other potential factors contributing to recent increase
2. interacting extremes in a warming climate.
3. What's up with the different signal over Southern Europe, Mean vs Cold
4. Why is it wet-warm in central Europe but cold-dry in southern / Northen Europe (Hypothesis: westerly flow of moist, warm oceanic air in central Europe while weakened westerly flow further south leaves area open to easterly cold air inflow).

Acknowledgments

The ERA5 data used here is freely available from the Copernicus Climate Change Service. KK was partially supported by the NSF project NSF AGS-1934358 and by the NOAA RISA Program award NA20OAR4310147A. GM has received funding from the European Research Council (ERC) under the European Union's Horizon 2020 research and innovation programme (Grant agreement No. 948309, CENÆ Project), and was partly supported by the Swedish Research Council Vetenskapsrådet, grant no. 2016-03724.

References

Amores, A., Marcos, M., Carrió, D. S., & Gómez-Pujol, L. (2020). Coastal impacts of storm gloria (january 2020) over the north-western mediterranean. *Natural Hazards and Earth System Sciences*, *20*(7), 1955–1968.

Barnes, E. A., & Screen, J. A. (2015). The impact of arctic warming on the midlatitude jet-stream: Can it? has it? will it? *Wiley Interdisciplinary Reviews: Climate Change*, *6*(3), 277–286.

Blöschl, G., Hall, J., Parajka, J., Perdigão, R. A., Merz, B., Arheimer, B., ... others (2017). Changing climate shifts timing of european floods. *Science*, *357*(6351), 588–590.

Busby, J. W., Baker, K., Bazilian, M. D., Gilbert, A. Q., Grubert, E., Rai, V., … Webber, M. E. (2021). Cascading risks: Understanding the 2021 winter blackout in texas. *Energy Research & Social Science*, *77*, 102106.

Cattiaux, J., Peings, Y., Saint-Martin, D., Trou-Kechout, N., & Vavrus, S. J. (2016). Sinuosity of midlatitude atmospheric flow in a warming world. *Geophysical Research Letters*, *43*(15), 8259–8268.

Ciric, D., Nieto, R., Losada, L., Drumond, A., & Gimeno, L. (2018). The mediterranean moisture contribution to climatological and extreme monthly continental precipitation. *Water*, *10*(4), 519.

Cohen, J., Agel, L., Barlow, M., Garfinkel, C. I., & White, I. (2021). Linking arctic variability and change with extreme winter weather in the united states. *Science*, *373*(6559), 1116–1121.

Cohen, J., Screen, J. A., Furtado, J. C., Barlow, M., Whittleston, D., Coumou, D., … others (2014). Recent arctic amplification and extreme mid-latitude weather. *Nature geoscience*, *7*(9), 627–637.

Cohen, J., Zhang, X., Francis, J., Jung, T., Kwok, R., Overland, J., … others (2020). Divergent consensuses on arctic amplification influence on midlatitude severe winter weather. *Nature Climate Change*, *10*(1), 20–29.

Doss-Gollin, J., Farnham, D. J., Lall, U., & Modi, V. (2021). How unprecedented was the february 2021 texas cold snap? *Environmental Research Letters*, *16*(6), 064056.

Forzieri, G., Bianchi, A., e Silva, F. B., Herrera, M. A. M., Leblois, A., Lavalle, C., … Feyen, L. (2018). Escalating impacts of climate extremes on critical infrastructures in europe. *Global environmental change*, *48*, 97–107.

Fragkoulidis, G., & Wirth, V. (2020). Local rossby wave packet amplitude, phase speed, and group velocity: Seasonal variability and their role in temperature extremes. *Journal of Climate*, *33*(20), 8767–8787.

Gao, Y., Leung, L. R., Lu, J., & Masato, G. (2015). Persistent cold air outbreaks over north america in a warming climate. *Environmental Research Letters*, *10*(4), 044001.

Grotjahn, R., Black, R., Leung, R., Wehner, M. F., Barlow, M., Bosilovich, M., … others (2016). North american extreme temperature events and related large scale meteorological patterns: a review of statistical methods, dynamics, modeling, and trends. *Climate Dynamics*, *46*(3), 1151–1184.

Hales, S., Edwards, S., & Kovats, R. (2003). Impacts on health of climate extremes. In A. J. McMichael et al. (Eds.), *Climate change and human health: risks and responses* (p. 79-102). World Health Organisation.

Harnik, N., Messori, G., Caballero, R., & Feldstein, S. B. (2016). The circumglobal north american wave pattern and its relation to cold events in eastern north america. *Geophysical Research Letters*, *43*(20), 11–015.

Hersbach, H., Bell, B., Berrisford, P., Hirahara, S., Horányi, A., Muñoz-Sabater, J., … others (2020). The era5 global reanalysis. *Quarterly Journal of the Royal Meteorological Society*, *146*(730), 1999–2049.

Kornhuber, K., Coumou, D., Vogel, E., Lesk, C., Donges, J. F., Lehmann, J., & Horton, R. M. (2020). Amplified rossby waves enhance risk of concurrent heatwaves in major breadbasket regions. *Nature Climate Change*, *10*(1), 48–53.

Kornhuber, K., Osprey, S., Coumou, D., Petri, S., Petoukhov, V., Rahmstorf, S., & Gray, L. (2019). Extreme weather events in early summer 2018 connected by a recurrent hemispheric wave-7 pattern. *Environmental Research Letters*, *14*(5), 054002.

Kretschmer, M., Coumou, D., Agel, L., Barlow, M., Tziperman, E., & Cohen, J. (2018). More-persistent weak stratospheric polar vortex states linked to cold extremes. *Bulletin of the American Meteorological Society*, *99*(1), 49–60.

López-Bueno, J., Linares, C., Sánchez-Guevara, C., Martinez, G., Mirón, I., Núñez-Peiró, M., ... Díaz, J. (2020). The effect of cold waves on daily mortality in districts in madrid considering sociodemographic variables. *Science of the total environment*, *749*, 142364.

Martin, J. E. (2021). Recent trends in the waviness of the northern hemisphere wintertime polar and subtropical jets. *Journal of Geophysical Research: Atmospheres*, *126*(9), e2020JD033668.

Matthias, V., & Kretschmer, M. (2020). The influence of stratospheric wave reflection on north american cold spells. *Monthly Weather Review*, *148*(4), 1675–1690.

MunichRe. (2020). *The natural disaster figures for 2020* (Tech. Rep.).

Musselman, K. N., Lehner, F., Ikeda, K., Clark, M. P., Prein, A. F., Liu, C., ... Rasmussen, R. (2018). Projected increases and shifts in rain-on-snow flood risk over western north america. *Nature Climate Change*, *8*(9), 808–812.

Rajczak, J., & Schär, C. (2017). Projections of future precipitation extremes over europe: A multimodel assessment of climate simulations. *Journal of Geophysical Research: Atmospheres*, *122*(20), 10–773.

Raymond, C., Horton, R. M., Zscheischler, J., Martius, O., AghaKouchak, A., Balch, J., ... others (2020). Understanding and managing connected extreme events. *Nature climate change*, *10*(7), 611–621.

Scoccimarro, E., Gualdi, S., Bellucci, A., Zampieri, M., & Navarra, A. (2013). Heavy precipitation events in a warmer climate: Results from cmip5 models. *Journal of climate*, *26*(20), 7902–7911.

Screen, J. A. (2014). Arctic amplification decreases temperature variance in northern mid-to high-latitudes. *Nature Climate Change*, *4*(7), 577–582.

Screen, J. A., & Simmonds, I. (2014). Amplified mid-latitude planetary waves favour particular regional weather extremes. *Nature Climate Change*, *4*(8), 704–709.

Sefton, C., Muchan, K., Parry, S., Matthews, B., Barker, L., Turner, S., & Hannaford, J. (2021). The 2019/2020 floods in the uk: a hydrological appraisal. *Weather*.

Sillmann, J., Croci-Maspoli, M., Kallache, M., & Katz, R. W. (2011). Extreme cold winter temperatures in europe under the influence of north atlantic atmospheric blocking. *Journal of Climate*, *24*(22), 5899–5913.

Singh, D., Swain, D. L., Mankin, J. S., Horton, D. E., Thomas, L. N., Rajaratnam, B., & Diffenbaugh, N. S. (2016). Recent amplification of the north american winter temperature dipole. *Journal of Geophysical Research: Atmospheres*, *121*(17), 9911–9928.

Smith, E. T., & Sheridan, S. C. (2019). The influence of extreme cold events on mortality in the united states. *Science of the Total Environment*, *647*, 342–351.

Teng, H., Branstator, G., Wang, H., Meehl, G. A., & Washington, W. M. (2013). Probability of us heat waves affected by a subseasonal planetary wave pattern. *Nature Geoscience*, *6*(12), 1056–1061.

Vajda, A., Tuomenvirta, H., Juga, I., Nurmi, P., Jokinen, P., & Rauhala, J. (2014). Severe weather affecting european transport systems: the identification, classification and frequencies of events. *Natural hazards*, *72*(1), 169–188.

Wirth, V., Riemer, M., Chang, E. K., & Martius, O. (2018). Rossby wave packets on the midlatitude waveguide—a review. *Monthly Weather Review*, *146*(7), 1965–2001.

Woollings, T., Barriopedro, D., Methven, J., Son, S.-W., Martius, O., Harvey, B., ... Seneviratne, S. (2018). Blocking and its response to climate change. *Current climate change reports*, *4*(3), 287–300.

Zscheischler, J., Martius, O., Westra, S., Bevacqua, E., Raymond, C., Horton, R. M., ... others (2020). A typology of compound weather and climate events. *Nature reviews earth & environment*, *1*(7), 333–347.

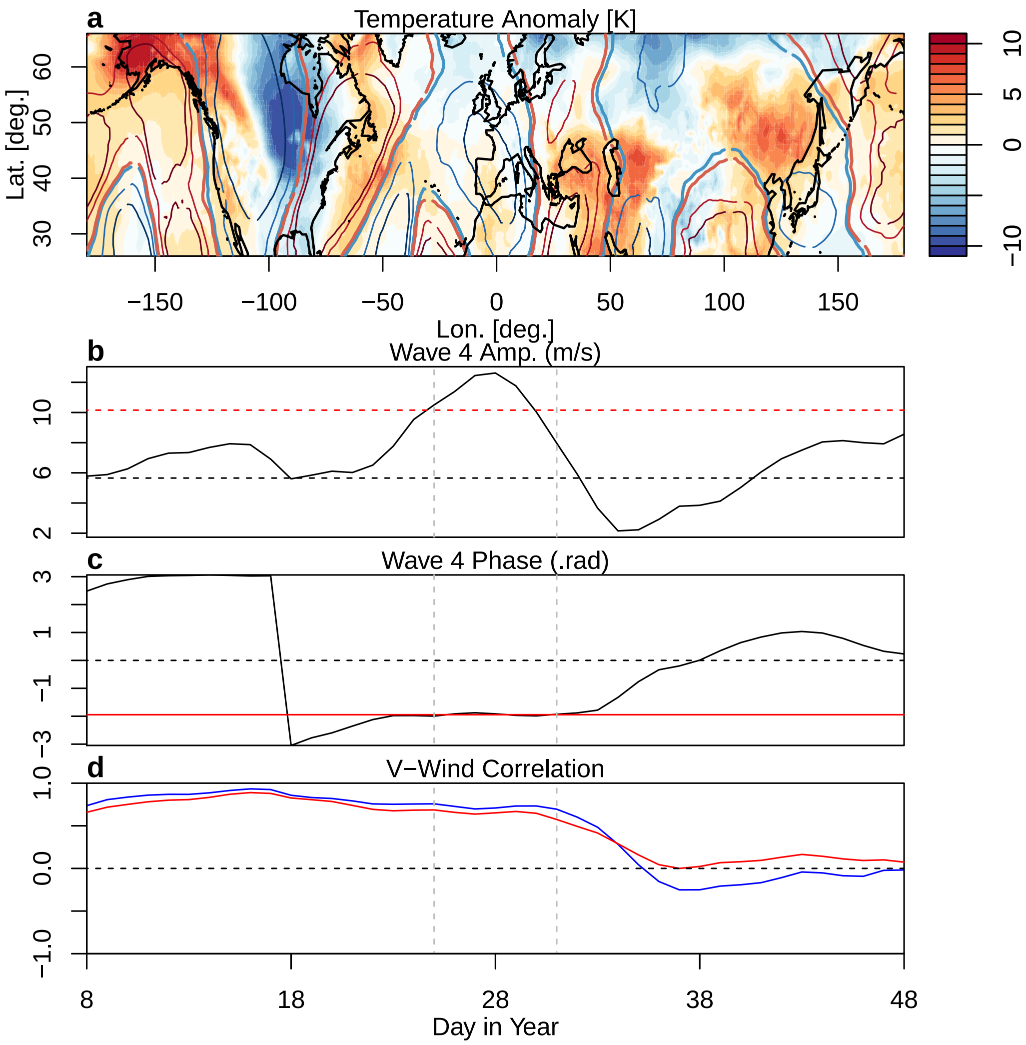

Figure 1. The extreme January-February cold spell of 2019. (a) Temperature Anomalies and 250 mb meridional wind fields (line contours; red: North-South, blue: South-North) in the northern hemisphere averaged over 7 days centered around the 28th of January 2019 (grey dashed vertical lines in (b-d). (b) Wave-4 amplitude (m/s) from January 8th - February 20th 2019. Average values are provided by the black dashed line while the 1.5std above and below mean are indicated by red dashed horizontal lines. (c) Wave 4 phase (rad) over the same timeperiod, the wave remains stationary throughout the indicated period. (d) pattern correlation over the North Atlantic sector (Fig. 3a (30–72.5 °N, 160 °W–40 °E).

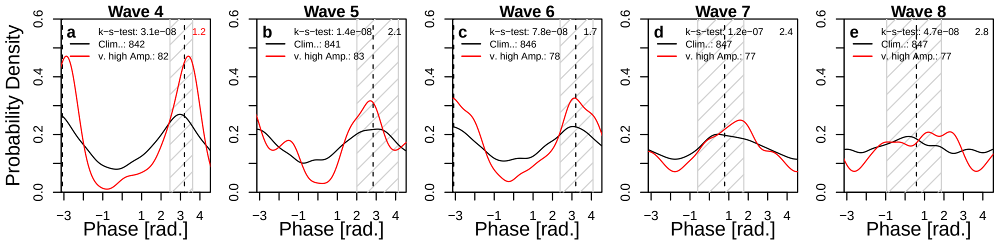

Figure 2. Density distributions of waves 4-8 during weeks of high amplitude (red) and all other weeks (black) detected in NDJFM 1979-2019. Grey hatching shows the area within the 25th -75th percentile (width in .rad provided in upper right corner), while the dashed black lines denote the median phase position during high amplitude events. The p-value from a Kolmogorov - Smirnov test is provided in the upper left above the sample size of each distribution. Wave-4 shows the strongest phase locking behaviour with a confined single peak and is the only wave meeting the phase locking definition from Kornhuber et al. (2020) (width ¡ pi/2). Note that the x-axes extended beyond pi to provide a continuous depiction of the distributions.

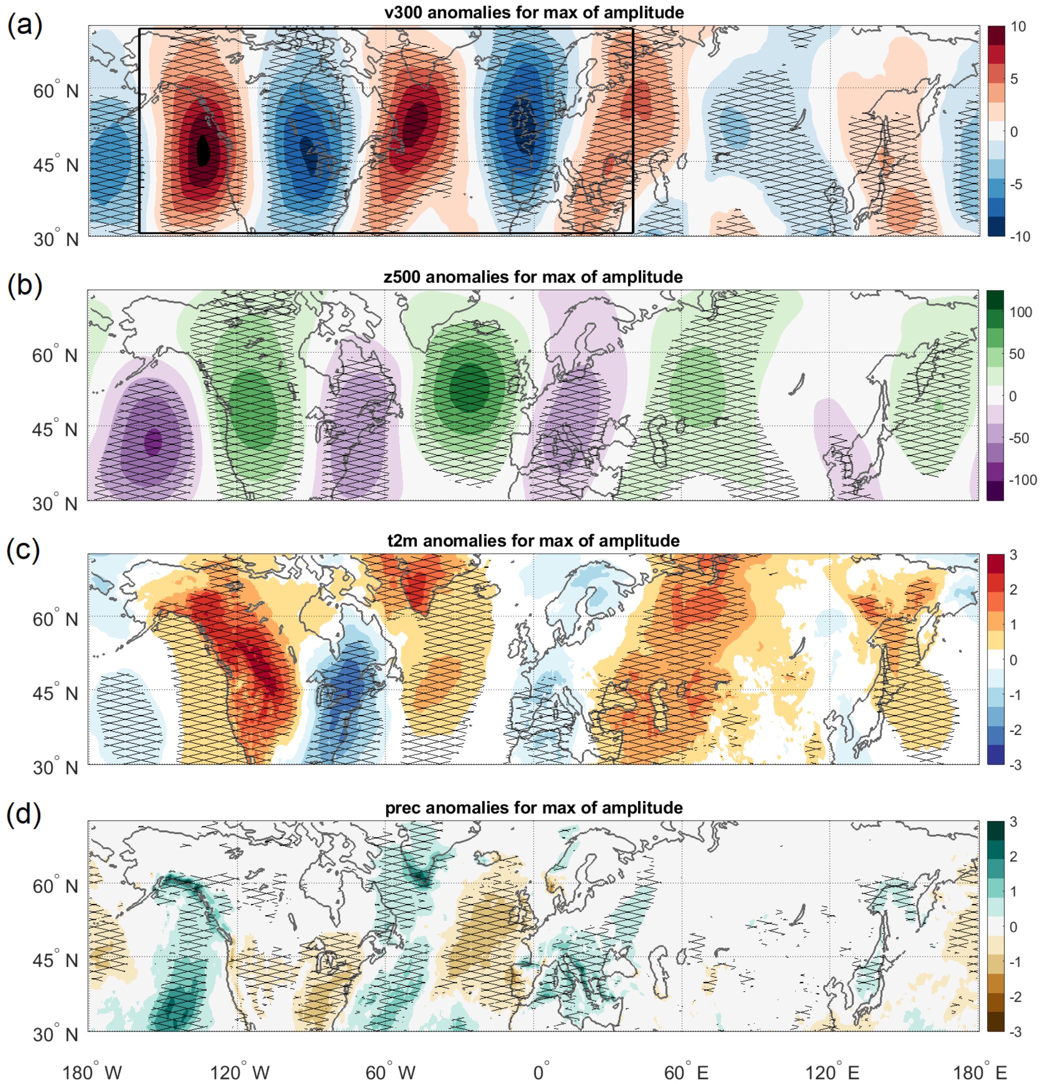

Figure 3. A recurrent wave pattern in the NH November-March circulation and associated surface conditions: Composites of the (a) 250 hpa meridional wind ($m\ s^{-1}$), (b) 500 hPa geopotential height (m), (c) 2-metre temperature (K) and (d) precipitation ($mm\ day^{-1}$) anomaly fields during wave-4 amplitude events (N=82). Anomalies significant at the 2-sided 5% level are cross-hatched. The black box in (a) illustrates the Pan-Atlantic domain 30–72.5 °N, 160 °W–40 °E by which wave phase events are determined (see Fig. SI wave phase events) .

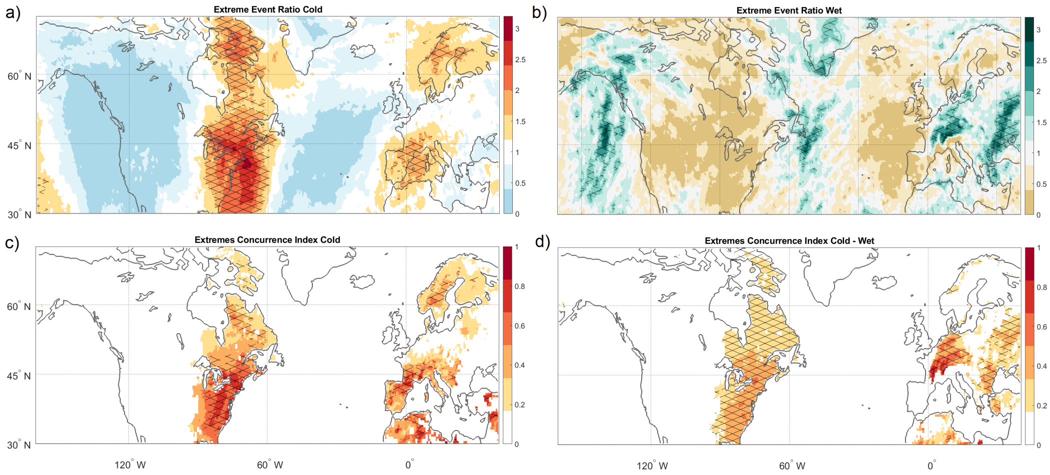

Figure 4. Amplifying effect of wave-4 on regional and concurrent of cold and wet extremes over the Pan-Atlantic sector. November-March ratio of extreme (a) cold and (b) heavy precipitation events during days displaying peak correlation in the North-American – European sector (see black box in Fig. 3a) relative to climatology. Concurrent extremes quantified by ECI for (c) cold extremes over NA and Europe and (d) cold extremes over NA and wet extremes over Europe. Hatching shows one-sided 5% significance. Fields correspond to the 5 days centred around the day for which a peak pattern correlation is identified.

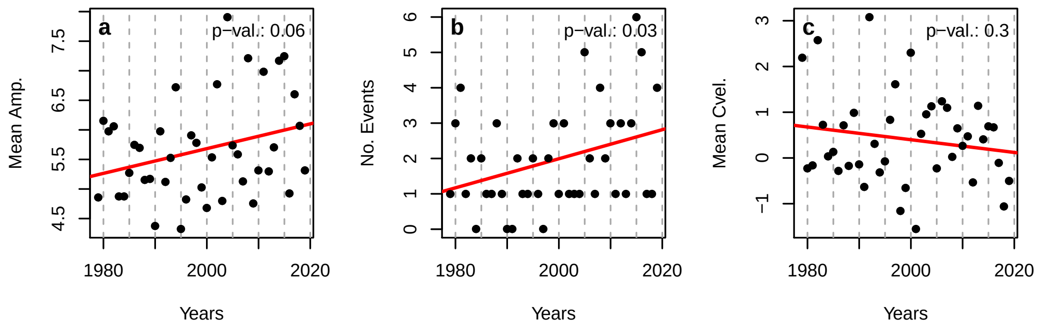

Figure 5. Annual trends in (a) mean wave amplitude, (b) wave amplitude events and (c) average phase velocity in the NH cold season (NDJFM, 1979-2019). Trends are quantified by a linear regression (solid red lines). Significant increases are identified for wave-amplitude and amplitude events, see p-value in the upper right of each panel.